Earth and Space Science

RESEARCH ARTICLE
10.1029/2022EA002571

Spatiotemporal Analysis of Extreme Temperature Change on the Tibetan Plateau Based On Quantile Regression

Ling Yao[1,2], Jiaying Lu[1,3], Wenjie Zhang[1,4], Jun Qin[1,3], Chenghu Zhou[1,3], Ngoc Nguyen Tran[5,6], and Ekena Rangel Pinagé[6,7]

[1]State Key Laboratory of Resources and Environmental Information System, Institute of Geographic Sciences and Natural Resources Research, Chinese Academy of Sciences, Beijing, China, [2]Jiangsu Center for Collaborative Innovation in Geographical Information Resource Development and Application, Nanjing Normal University, Nanjing, China, [3]College of Resources and Environment, University of Chinese Academy of Sciences, Beijing, China, [4]School of Geographical Sciences, Nanjing University of Information Science & Technology, Nanjing, China, [5]School of Information and Communication Technology, Hanoi University of Science and Technology, Hanoi, Vietnam, [6]School of Life Science, University of Technology Sydney, Ultimo, NSW, Australia, [7]College of Forestry, Oregon State University, Corvallis, OR, USA

Key Points:

- Changes in temperature extremes are comprehensively investigated based on quantile regression over the Tibetan Plateau (TP)
- The entire density function of the daily temperature time-series was built by quantile regression
- The mechanisms and altitude dependence of climate warming was explored based on the trend retrieved by quantile regression

Correspondence to:
W. Zhang,
zhangwenjie@nuist.edu.cn

Citation:
Yao, L., Lu, J., Zhang, W., Qin, J., Zhou, C., Tran, N. N., & Pinagé, E. R. (2022). Spatiotemporal analysis of extreme temperature change on the Tibetan Plateau based on quantile regression. *Earth and Space Science*, *9*, e2022EA002571. https://doi.org/10.1029/2022EA002571

Received 14 AUG 2022
Accepted 29 SEP 2022

Author Contributions:

Methodology: Ling Yao, Jiaying Lu, Jun Qin
Supervision: Wenjie Zhang, Jun Qin, Chenghu Zhou
Visualization: Jiaying Lu
Writing – original draft: Ling Yao
Writing – review & editing: Wenjie Zhang, Ngoc Nguyen Tran, Ekena Rangel Pinagé

Abstract

Temperature extremes have been extensively observed on the Tibetan Plateau (TP), of which the dynamics were mostly monitored by traditional trend analysis based on linear regression. This method however, is often impacted by a quasi-periodic heterogeneity disturbance in variance, leading to results susceptible to extreme outliers. In this study, we conducted the comprehensive detection of extreme temperature changes using quantile regression on the TP from 100 weather stations from 1979 to 2019. The use of quantile regression enabled us to characterize the entire density function of the extreme temperature time-series (the daily minimum, mean and maximum temperature) at each location. Our results revealed that the daily minimum temperature was generally warming faster than the daily maximum and mean temperatures with the respective trend interval of [−0.45, 1.29], [−0.1, 0.98], [−0.01, 1.01] °C/decade among the conditional quantile levels. Furthermore, the warming rate of extremely cold (0.05 quantile level) and hot days (0.95 quantile level) was higher than that of the mean condition (0.5 quantile level) in each extreme temperature time-series. We also found that there was a significant elevation-dependent warming only in extremely cold days. In addition, results from the teleconnection analysis showed that the Arctic Oscillation had a strong influence on the extreme cold and hot extremes over the northern and southwestern TP region, while the El Niño-Southern Oscillation mainly modulated temperatures over the southeastern TP area. This study can potentially offer improved understanding of the temperature extremes over TP in the face of global warming.

Plain Language Summary

It is well known that the Tibetan Plateau (TP) is covered extensively with snow and ice and is the major birthplace of many Asian rivers and nurtures billions of people. In the context of global warming, extreme temperature events were found to be more frequent and intense, which has posed increasing threats to the hydrological ecosystem over TP. Although the changes in temperature extremes over the TP have been previously investigated, these studies mostly applied traditional linear regression, which is sensitive and vulnerable to extreme outliers and serial correlation. Therefore, this study aimed to obtain reliable trends in temperature extremes based on a quantile regression method, along with an in-depth understanding of their elevation dependency. By investigating daily minimum, mean and maximum temperatures at 100 stations, our results showed that significant and universal warming occurred at most stations. Moreover, extreme minimum temperatures usually changed faster than extreme maximum temperatures, which was also true for extremely cold (low quantile group) and hot days (high quantile group) in the same variable. Additionally, it was evidenced that there was a significant elevation-dependent warming only on extremely cold days.

1. Introduction

In the context of global warming, mountains and high-latitude areas are getting more attention because of their rapid warming rate (Lan et al., 2022; Pepin et al., 2015; Screen, 2014). The Tibetan Plateau (TP), with an elevation of over 4,000 m above sea level, has experienced substantial warming even in the so-called "warming hiatus" period (Duan & Xiao, 2015; Yin et al., 2019; You, Kang, Aguilar, et al., 2008, You, Kang, Pepin, et al., 2008). Rapid warming has exerted a huge impact on the fragile ecosystems of the TP, including rapid glacier melting

(Yao et al., 2012; Zhang et al., 2014, 2016), vegetation migration (Yan & Tang, 2019) and a deterioration in the landscape quality (Fan et al., 2021). Moreover, the increased frequency of natural disasters associated with climate warming has raised the threats to people's lives and property on the TP (Cui et al., 2014).

Associated with the dramatic warming, extreme weather and climate events have occurred with increasing frequency on the TP in recent decades, therefore, the studies identifying climate trends in temperature extremes have significantly progressed over the TP during multiple temporal periods (Ding et al., 2018; Li et al., 2010; Liu et al., 2006, 2011; Wang et al., 2013; Xue et al., 2020; You, Kang, Aguilar, et al., 2008, You, Kang, Pepin, et al., 2008). However, the majority of the analysis undertaken on the TP are based on the monthly composited or annually composited daily extremes. For instance, the increase trend of annual-mean daily minimum and maximum temperature are 0.41 and 0.18°C/decade during 1961–2003 (Liu et al., 2006), 0.51 and 0.28°C/decade during 1961–2007 (Li et al., 2010), 0.41 and 0.25°C/decade during 1970–2005 (Liu et al., 2011), respectively. The averaged extreme temperatures are highly likely to smooth out a lot of the key information. On the other hand, the methodology for trend identification involved in the studies mentioned used linear regression, which is sensitive and vulnerable to extreme outliers and serial correlation (Duan et al., 2021; Gao & Franzke, 2017). As an alternative to linear regression, quantile regression does not require the strict assumption that the residuals normally distributes in the regression. Compared to linear regression, quantile regression is more robust, especially when extreme outliers are contained, a key feature when investigating temperature extremes (Franzke, 2013). and all de-seasonalized daily temperature extremes can be used to build the conditional quantile functions. The idea was first proposed by Koenker and Bassett (1978), and then played a great role particularly for in trend identifications of any percentiles of temperature (Barbosa et al., 2011; Duan et al., 2021; Franzke, 2013; Gao & Franzke, 2017; Koenker & Schorfheide, 1994). Its proved its performance is reliable in comparison with robust linear regression and the nonparametric M-K test (Gao & Franzke, 2017). Nevertheless, few studies have applied quantile regression to the extreme temperatures change on the TP, especially when investigating the daily maximum, minimum, and mean temperatures at the same time. The other advantage of this approach is that the conditional quantile functions allow us to analyze the relationship at differently conditional-distributed points based on central tendency and statistical dispersion in the various measures.

The reliable trend's estimates from quantile function allow us to deeply investigate altitude dependence of climate warming on the TP. Liu et al. (2009) found significant elevation dependence on the TP in annual-composited daily minimum temperatures of either meteorological observations or simulations during 1961–2006, while many other studies revealed that there was no elevation-dependent change in both extreme warm and cold indices during 1961–2005 (You, Kang, Pepin, et al., 2008). In quantile regression, the lower and higher quantile grounds can reveal changes in extremely cold days and extremely hot days among temperature variables (Gao & Franzke, 2017), which can further enhance the exploration of warming change with elevation. Additionally, quantile regression can also be employed to detect the teleconnections between warming extremes and large-scale climate patterns. Recent findings suggest that, in China, the El Niño–Southern Oscillation (ENSO) has the potential to affect the variability of extreme temperatures during summer in eastern China (Chen et al., 2013). The Arctic Oscillation (AO) is one of the major factors influencing climate variability in the Northern Hemisphere (Feldstein & Franzke, 2017), and it is most pronounced in winter and in mid- and high-latitudes regions (Ramos et al., 2010). Correlation analysis manifested a strong positive relationship between winter temperature extremes and the AO over northern China (Gong & Wang, 2003; You et al., 2011), however, to the best of our knowledge, the teleconnections have not been well investigated on the TP in combination with quantile regression.

The objectives of this study are, therefore, to (a) deepen the understanding of the extreme temperature changes from 1979 to 2019 on the TP based on quantile regression, including the daily minimum (T_{min}), mean (T_{avg}) and maximum temperature (T_{max}); (b) future investigate the change of extremely hot days and extremely hot days in each extreme temperature based on the entire density function of the daily temperature time-series built by quantile regression (c) explore mechanisms by connections between extreme temperatures and two large-scale climate patterns and the altitude dependence of extreme temperature changes.

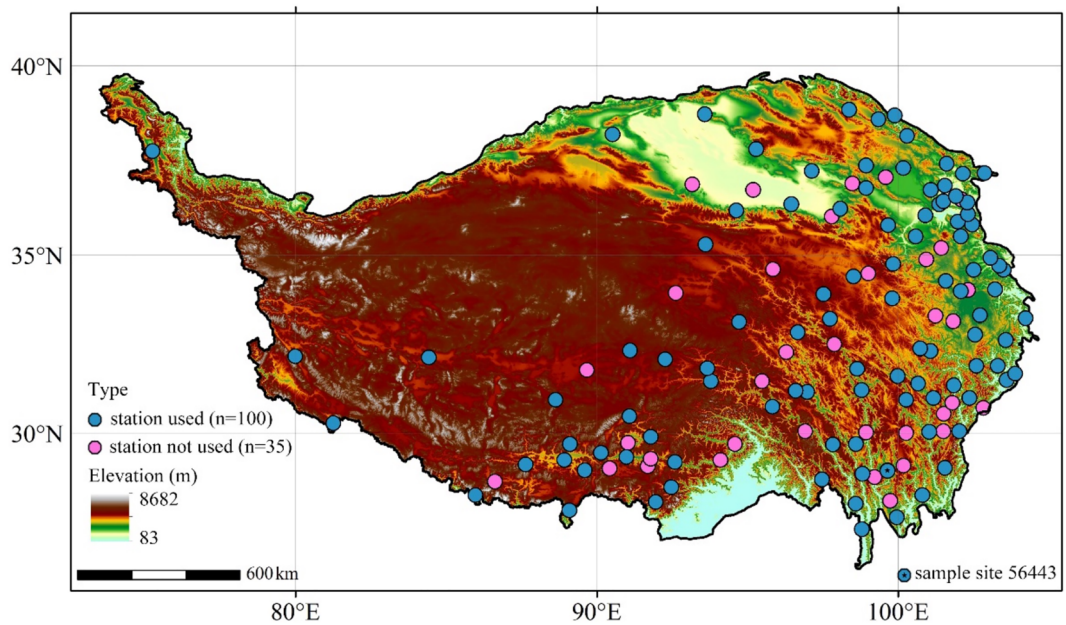

Figure 1. Geographical distribution of meteorological stations on Tibetan Plateau (TP). Stations in blue color indicate the meteorological stations used in this study and red ones means the exclusions.

2. Materials and Methods

2.1. Data of Meteorological Observation and Climate Patterns

The temperature data at 135 meteorological stations from 1979 to 2019 on the TP is obtained from the Daily Data set of Basic Meteorological Elements of National Surface Meteorological Stations in China (National Meteorological Information Center, 2019), which can be accessed through the depository link of https://agupubs.onlinelibrary.wiley.com/doi/full/10.1029/2022EA002232. Thirty-five sites are excluded in the analysis because of the replacement of equipment or because of discontinuous observations. The specific spatial distribution of sites involved in this study is shown in Figure 1. In view of the significant influence of seasonality, the classical de-seasonalization approach is adopted for T_{min}, T_{avg}, and T_{max}, respectively (Fatichi et al., 2009). First, an observed time series X_t is divided into 365 subseries, which is constructed with the available daily data of the year. For every subseries, mean and variance are calculated, generating 365 values of mean and variance function of the Julian day. The seasonality in each X_t is then erased through subtracting the mean and then dividing by the standard deviation of the same day (Grimaldi, 2004). Moreover, to reveal the drivers of climate change on the TP, the teleconnection in daily scale between climate extremes and large-scale climate patterns is analyzed by quantile regression. The climate extremes of ENSO and AO are considered in view of their significant impact that has been proven in China (Chen et al., 2013; Gao & Franzke, 2017; Kenyon & Hegerl, 2008). The data of ENSO and AO can be accessed through the depository link of https://www.psl.noaa.gov/data/gridded/data.noaa.oisst.v2.highres.html and https://www.cpc.ncep.noaa.gov/products/precip/CWlink/daily_ao_index/ao.shtml, respectively.

2.2. The Detection of Long-Range Dependence

Long-range dependence (hereafter LRD) means auto-correlation between distant observations of a time series which is likely to exist in the trend of a daily temperature series, which can induce trend like behaviors and increase the statistical uncertainty in trend detection (Franzke, 2012, 2013). Therefore, the priority is to examine the evidence of LRD for T_{min}, T_{avg}, and T_{max}. The Auto-Regressive Fractionally Integrated Moving Average model (ARFIMA (p, d, q)), which is proven as one the most flexible models (Granger & Joyeux, 1980; Hosking, 1981),is able to simulate the long memory autocorrelation structure and a stationary normal time series by a linear random model. The output parameter d in the simulation is generally regarded as the strength of long-range correlation. There are a number of methods that can be used to investigate LRD and to estimate the parameter d through

Table 1
Description of the Nine Temperature Indices Selected for the Analysis Based on the Deseasonalized-Daily Temperature Serial From 1979 to 2019

Label	Definition	Units
T_{min}	The daily minimum temperature time series	°C
T_{avg}	The daily mean temperature time series	°C
T_{max}	The daily maximum temperature time series	°C
$T_{min\_0.05}$	The trend of the daily minimum temperature serial at 0.05 quantile level	°C/decade
$T_{min\_0.5}$	The trend of the daily minimum temperature serial at 0.5 quantile level	°C/decade
$T_{min\_0.95}$	The trend of the daily minimum temperature serial at 0.95 quantile level	°C/decade
$T_{avg\_0.05}$	The trend of the daily mean temperature serial at 0.05 quantile level	°C/decade
$T_{avg\_0.5}$	The trend of the daily mean temperature serial at 0.5 quantile level	°C/decade
$T_{avg\_0.95}$	The trend of the daily mean temperature serial at 0.95 quantile level	°C/decade
$T_{max\_0.05}$	The trend of the daily maximum temperature serial at 0.05 quantile level	°C/decade
$T_{max\_0.5}$	The trend of the daily maximum temperature serial at 0.5 quantile level	°C/decade
$T_{max\_0.95}$	The trend of the daily maximum temperature serial at 0.95 quantile level	°C/decade

either parametric or non-parametric methods. In this study, a semiparametric approach proposed by Geweke and Porter-Hudak (hereafter GPH method) is adopted to detect the parameter d and the corresponding significance test of 95% confidence interval (Geweke & Porter-Hudak, 1983). If 0 is not in the 95% confidence interval, d is viewed as significant.

2.3. Trend Analysis and Significance Test

In this study, quantile regression is applied to identify the trend of the temperature variables of T_{min}, T_{avg}, and T_{max} at quantile levels of 0.05, 0.5, and 0.95 (Table 1). The quantile levels of 0.05, 0.5, and 0.95 can also be viewed as the extremely cold days, the mean condition and the extremely hot days. Quantile regression is robust against outliers relative to traditional linear regression, which highlights its ability in the trend detection of the extremes, furthermore, different measures of central tendency and statistical dispersion generated by conditional quantile function can process a comprehensive analysis between explanatory variables. Similarly, the use of least squares to determine ordinary linear regression, the essence of quantile regression can be reduced to the solution of minimization problem (Franzke, 2013). There is evidence that linear, quadratic, and cubic quantile regression can obtain similar trends over China (Gao & Franzke, 2017), hence, only linear quantile regression is applied in this study for simplicity purposes. Linear quantile regression is based on minimizing the weighted residual sum of mean absolute difference (MAD), shown as Equations 1 and 2.

$$Q_\tau(y_i) = \beta_0(\tau) + \beta_1(\tau)x_{i1} + \ldots + \beta_p(\tau)x_{ip} \tag{1}$$

$$\text{MAD} = \frac{1}{n}\sum_{i=1}^{n} \rho_\tau(y_i - (\beta_0(\tau) + \beta_1 x_{i1}(\tau) + \ldots + \beta_p x_{ip}(\tau)))^2 \tag{2}$$

where, Q represents the corresponding conditional quantile, y represents response variable, $x_{i1},\ldots,x_{ip}$ represent independent variables, i equals 1, 2, .., n. And p represents the number of regression variables, τ represents the quantile level, β is a function of τ and is estimated by minimizing MAD, the function ρ is referred to as the check loss, n is the number of data points.

To reveal the extreme trend symmetry in each variable, the trend estimated from the 0.5 quantile is chose as the reference, as illustrated in Equations 3 and 4.

$$\text{Trend}_{cold} = \text{Trend}(\tau = 0.05) - \text{Trend}(\tau = 0.5) \tag{3}$$

$$\text{Trend}_{hot} = \text{Trend}(\tau = 0.95) - \text{Trend}(\tau = 0.5) \tag{4}$$

where, $\text{Trend}_{\text{cold}}$ and $\text{Trend}_{\text{hot}}$ represent extremely cold or hot days relative to mean condition of each temperature variable.

Next, the surrogate data generating method proposed by Schreiber and Schmitz (1996) is adopted to test the statistical significance of the quantile trend. Surrogate time series generated by this method need to meet the prerequisites of the same autocorrelation and probability density function. Here we generate 1,000 sets of such data for each quantile of T_{min}, T_{avg}, and T_{max}. The quantile trends of the observed time series are considered statistically significant as they locate outside the 5% or 95% percentile distribution from the proxy data (Franzke, 2013).

2.4. Analysis of Elevation Dependent Warming, Spatial Cluster, and the Teleconnections

In this study, the relationship between elevation and the quantile trends (quantile levels $\tau = 0.05, 0.5, 0.95$) of T_{min}, T_{avg}, and T_{max} is separately explored by the ordinary linear regression. The topography data [Global 30 Arc-Second Elevation (GTOPO30)] was obtained from the U.S. Geological Survey (https://doi.org/10.5066/F7DF6PQS). To identify the spatial pattern of extreme temperature changes happening on the TP, the popular K-Nearest Neighbor (KNN) algorithm is adopted in view of its stability and high accuracy (Zhu et al., 2022). The quantile trends (quantile levels $\tau = 0.05, 0.5, 0.95$) of each temperature time series (a total of nine feature) are used as input to KNN and three clusters are restricted in the model. To further analyze the driving mechanisms behind the spatial clusters, the potential teleconnections between extreme temperature time series and ENSO and AO are respectively computed. It is worth emphasizing that the telecorrelations are carried out on a daily scale and all stations at the same cluster are utilized to calculate the teleconnections between daily extreme temperature variables at quantile levels of 0.05, 0.5, and 0.95 and climate index (ENSO and AO) respectively.

3. Results

3.1. Long-Range Dependence Test

The LRD of de-seasonalized daily temperature variables is examined at 100 selected stations on the TP by using the GPH method. Figure 2 shows the LRD values of T_{min} is generally greater than of T_{avg} and T_{max}, ranging from 0.13 to 0.50, 0.06 to 0.42 and 0.08 to 0.38 respectively (Table 2). Moreover, with respect to T_{min}, the d values at most of stations are significantly different from zero with the exception of those for five stations. However, the number of insignificant stations increases to 16 for T_{avg} and 19 for T_{max}, which are mainly located in the eastern TP. Figure 2 also shows that all d values of the three temperature variables are positive and less than 0.5 (Table 2), which indicates the daily temperature time series is persistent. LRD may induce trend-like behaviors and this section therefore demonstrates the necessity to consider it in the following trend analysis.

3.2. Quantile Trend Analysis and Significance Test

Figure 3 illustrates the details of quantile regression at station 56,443 (28.9°N, 99.65°E). Figure 4 shows the values of quantile regression trend of T_{min}, T_{avg}, and T_{max} at quantile levels of 0.05, 0.5, and 0.95, respectively. It manifests extreme temperatures change on the TP is dominated by warming. From low to high quantile levels, the number of meteorological stations with an up trend is respectively 94, 98, 99 for T_{min} and 99, 98, 100 for T_{avg} and 100, 99, 100 for T_{max}. Furthermore, there is a pronounced difference against the trend of different quantiles in each extreme temperatures time-series (Table 2). For T_{min}, from low to high quantile, the trend interval is [−0.45, 1.29], [−0.30, 0.99], and [−0.08, 1.02] °C/decade, respectively (Table 2 and Figures 4a–4c). $T_{\text{min\_0.05}}$ at stations is usually larger than that of $T_{\text{min\_0.5}}$ and $T_{\text{min\_0.95}}$, and the median value is 0.49, 0.45, 0.42°C/decade respectively (Table 2 and Figures 4a–4c). However, more stations sail through the significance test in $T_{\text{min\_0.5}}$ compared with those of $T_{\text{min\_0.05}}$ and $T_{\text{min\_0.95}}$ and their numbers are respectively 93, 82, and 68 (Table 2 and Figures 4a–4c). The warming trend gradually increases from east to west, and the stations with non-significant trend are mainly located in the southeast and southwest of the TP. For T_{avg}, the trend intervals of $T_{\text{avg\_0.05}}$, $T_{\text{avg\_0.5}}$, and $T_{\text{avg\_0.95}}$ range respectively from [−0.03, 0.92], [−0.1, 0.92], and [0.01, 0.98]°C/decade (Table 2 and Figures 4d–4f). It also shows the trend of $T_{\text{avg\_0.05}}$ at stations is generally greater than that of $T_{\text{avg\_0.5}}$ and $T_{\text{avg\_0.95}}$ with the median trend of 0.42, 0.38, and 0.39°C/decade, and the number of sites with significant trend is 77, 93, 62 respectively (Table 2 and Figures 4d–4f). The spatial pattern of the larger trend from east to west appears to remain for $T_{\text{avg\_0.05}}$, but becomes blurred for two other conditional quantiles. For T_{max}, the trend intervals of $T_{\text{max\_0.05}}$, $T_{\text{max\_0.5}}$, and

10.1029/2022EA002571

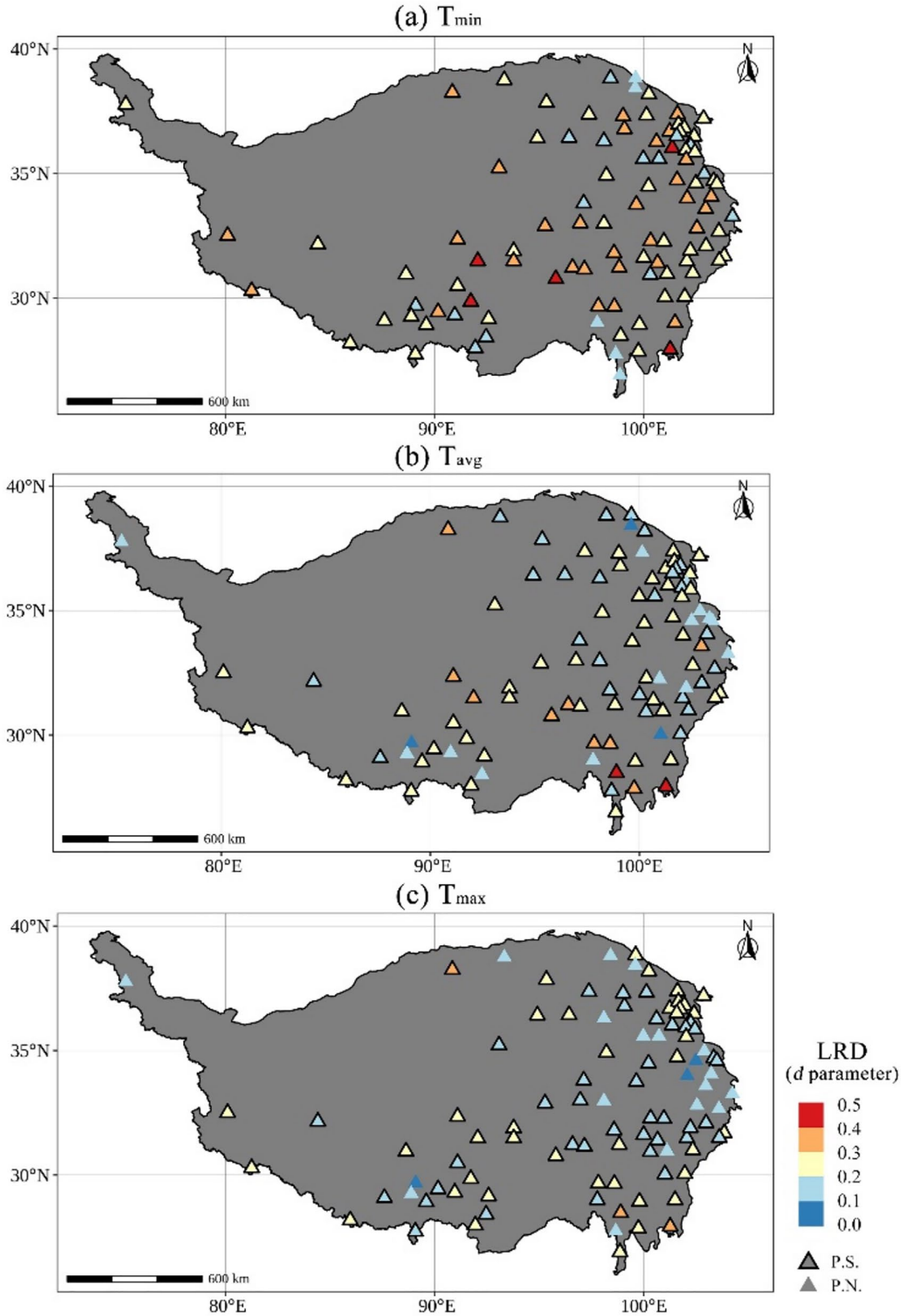

Figure 2. The parameter d of long-range dependence (LRD) for de-seasonalized daily temperature variables from 1979 to 2019 years, (a) T_{min}, (b) T_{avg}, (c) T_{max}. In legend, P.S. represents positive and significant trend at 0.05 significant level and P.N. represents positive and non-significant trend.

Table 2
Summary of Long-Range Dependence (LRD) and the Trend of Daily Minimum, Mean and Maximum Temperature Serial at Quantile Level τ = 0.05, 0.5, and 0.95 From 1979 to 2019

	Daily minimum temperature				Daily mean temperature				Daily maximum temperature			
	d	$\tau = 0.05$	$\tau = 0.5$	$\tau = 0.95$	d	$\tau = 0.05$	$\tau = 0.5$	$\tau = 0.95$	d	$\tau = 0.05$	$\tau = 0.5$	$\tau = 0.95$
Min	0.13	−0.45	−0.30	−0.08	0.06	−0.03	−0.10	0.01	0.08	0.03	−0.01	0.18
First quartile	0.21	0.29	0.32	0.32	0.16	0.32	0.28	0.28	0.16	0.34	0.33	0.37
Median	0.27	0.49	0.45	0.42	0.21	0.42	0.38	0.39	0.18	0.41	0.40	0.45
Mean	0.27	0.51	0.47	0.44	0.21	0.45	0.38	0.40	0.20	0.44	0.41	0.46
Third quartile	0.32	0.69	0.62	0.58	0.26	0.57	0.48	0.51	0.23	0.50	0.48	0.53
Max	0.50	1.29	0.99	1.02	0.42	0.93	0.92	0.98	0.38	0.93	1.01	0.98
Number of stations (trend>0)	/	94	98	99	/	99	98	100	/	100	99	100
Number of stations (significant)	/	82	93	68	/	77	93	62	/	60	83	81

$T_{max\_0.95}$ are [0.03, 0.93], [−0.01, 1.01], and [0.18, 0.98]°C/decade respectively (Table 2 and Figures 4g–4i) but the number of sites with non-significant trend sharply increases, especially for the extreme cold days and the extreme hot days. The stations with faster change trend are mainly distributed in the south-west area for $T_{max\_0.05}$ and at North-east area for $T_{max\_0.95}$. But the specific spatial pattern of larger trend from east to west becomes less visible on the TP.

The trend in the same quantile of different temperature variables also presents significant differences. For example, $T_{min\_0.05}$ generally changes faster than $T_{avg\_0.05}$ and $T_{max\_0.05}$ at most meteorological stations (Figures 4a, 4d and 4g) especially in the southwest region, where there is a cluster where $T_{max\_0.05}$ is faster than $T_{min\_0.05}$ and $T_{avg\_0.05}$. Moreover, the number of stations with non-significant $T_{max\_0.05}$ abruptly increases in the eastern TP. $T_{avg\_0.05}$ shows a similar pattern with $T_{min\_0.05}$ among different extreme temperatures time-series (Figures 4b, 4e and 4h) but stations with significant warming begins to spread to the southeastern TP. As for $T_{max\_0.05}$, a large number of non-significant stations are found on the TP for each extreme temperatures time-series, but the number for $T_{max\_0.95}$ is smaller than for $T_{min\_0.95}$ and $T_{avg\_0.95}$ (Figures 4c, 4f and 4i).

3.3. The Trend Asymmetry Between Extremely Cold and Hot Days

Figure 4 presents that the asymmetrical change of extremely cold and hot days relative to mean condition of each extreme temperatures time-series. Specifically, for T_{min} (Figure 5a), extremely cold days warms faster than extremely hot days at most sites. Only a small number of sites exclusively distribute in the northeastern and southern regions of TP. For T_{avg} (Figure 5b), a large number of sites with faster trend in extremely hot days appear on the eastern fringe area and on the south area of TP. And, its asymmetry is amplified compared with T_{min}. For T_{max} (Figure 5c), the spatial distribution of the asymmetry is similar to T_{avg}, while the asymmetry is further magnified on the eastern fringe area and on the south area of TP.

3.4. The Evidence of Elevation Dependence

To investigate the elevation dependence of extreme temperature change on elevation, the relationship between quantile regression trends of each variable and elevation is respectively calculated (Figure 6). For T_{min} (Figures 6a–6c), $T_{min\_0.05}$, $T_{min\_0.5}$, and $T_{min\_0.95}$, these all increase with elevation, while only $T_{min\_0.05}$ is significant (p-value < 0.05). For T_{avg} (Figures 6d–6f), $T_{avg\_0.05}$, $T_{avg\_0.5}$ remains positive with elevation, while $T_{avg\_0.95}$ becomes slight negative. The significance test indicates that only $T_{avg\_0.05}$ is significant. For T_{max} (Figures 6g–6i), the direction of the correlation and significant test is analogous with T_{avg}, while $T_{max\_0.95}$ decreases more rapid as altitude increasing.

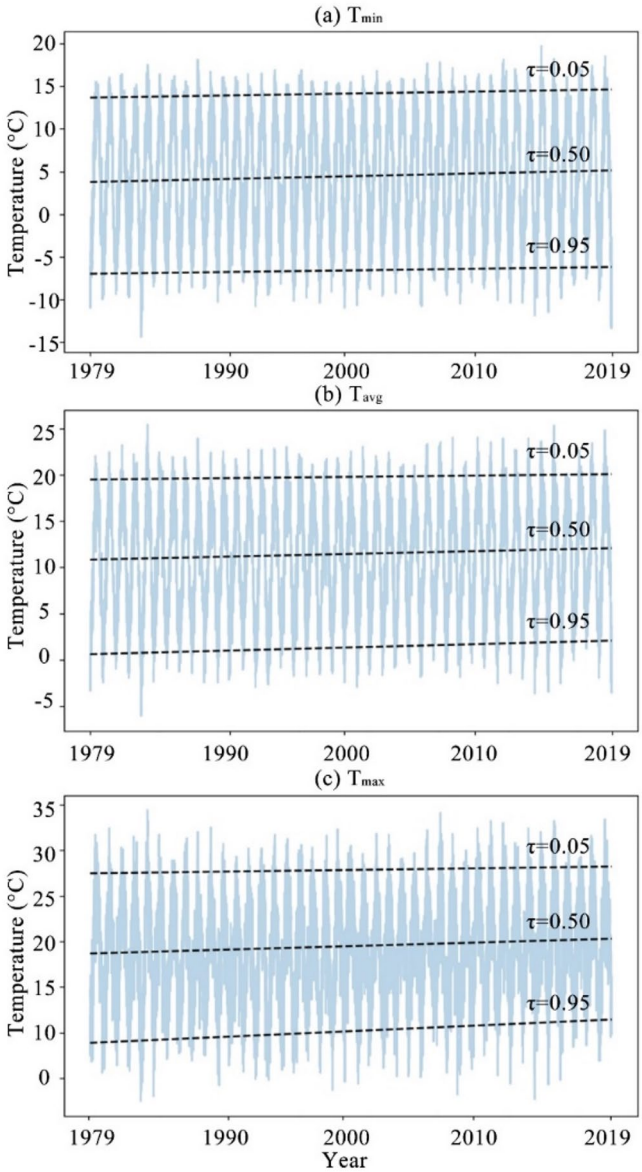

Figure 3. The quantile regression curves of daily temperatures at station 56,443 (28.9°N, 99.65°E) at quantile level 0.05, 0.50, and 0.95, (a) T_{min}, (b) T_{avg}, (c) T_{max}.

3.5. Spatial Cluster and the Driving Forces

To uncover the spatial pattern of extreme temperature change, the KNN algorithm is employed to analyze the spatial cluster vectors, simultaneously considering the quantile regression trends of T_{min}, T_{avg}, and T_{max} at following quantile levels: 0.05, 0.5, 0.95. As shown in Figure 7, three clusters with a specific pattern are discovered on the TP by the KNN algorithm. The largest cluster of C3 covering 68 stations is scattered across the north, west and middle area of TP. The cluster of C2 with 22 stations and C1 with 10 stations is mainly concentrated on the southeastern TP and on the southwestern TP, respectively.

To reveal the cause of extreme temperature changes, the potential teleconnections between the daily temperature time series and daily climate index of ENSO and AO in the three clusters are respectively computed by correlation analysis. Figures 7b–7d show that the ENSO index in the three clusters exhibits entirely negative correlations with all temperature time series at quantile levels of 0.05, 0.5, and 0.95. All of the correlations passed the significance test with the only exception for T_{min} at 0.95 quantile in C3 and for T_{max} at 0.5 quantile in C3. The comparably low correlation coefficients in C3 suggest that it is less likely to be influenced by El Niño. Meanwhile, El Niño appears to act mainly on extremely cold days (data at 0.05 quantile) and hot days (data at 0.95 quantile) of these temperature time series. The influence of the AO, appears to be more complicated in the three clusters. Figures 6e–6g indicate that the AO index generally has the negative correlations with the temperature time series for 0.05 and 0.5 quantile, but the direction is opposite for the 0.95 quantile. The correlation coefficients show that AO seems to have a larger impact on extremely cold and hot days, which is analogous with El Niño. Moreover, more clusters with non-significant correlation appears at the 0.5 quantile. The comparison between AO and ENSO shows that the absolute correlation coefficient of AO is higher than those of El Niño at the quantile level of 0.05 and 0.95, which implies a larger impact.

4. Discussion

4.1. Advantage of Quantile Regression

As the LRD will significantly increase the statistical uncertainty in the trend identification, detecting the existence of LRD is the preliminary and indispensable step to analyze the temperature extremes (Gao & Franzke, 2017). Many methods have been created to investigate the potential of LRD at global or regional scales (Franzke, 2012, 2013; Gao & Franzke, 2017). In this study, the semi-parametric method (GPH) (which has been successfully applied in previous studies (Franzke, 2010, 2012; Gao & Franzke, 2017)) is used to examine the evidence of LRD in the daily temperature series. Similarly, this study reveals that LRD is widely distributed on the TP. At 100 stations, the d values of 96, 84, and 81 stations in regard to T_{min}, T_{avg}, and T_{max} are significantly different from zero manifesting the universality of LRD on the TP (Figure 2 and Table 2). This also highlights that an appropriate method is required on the TP when testing the statistical significance of trends in extreme temperature. Climate extremes have been analyzed traditionally either on the basis of extreme climate indices (Alexander et al., 2006; You et al., 2011) or extreme value theory (Brown et al., 2008; Kharin et al., 2007, 2013). Quantile regression can further enrich the study of climate warming by investigating both the mean and extreme values (Franzke, 2013; Gao & Franzke, 2017). In this study, trends of T_{min}, T_{avg}, and T_{max} are comprehensively investigated over the TP based on quantile regression. Quantile levels of 0.05, 0.5, and 0.95 can represent the change of extremely cold days, mean days and extremely hot days respectively (Gao & Franzke, 2017).

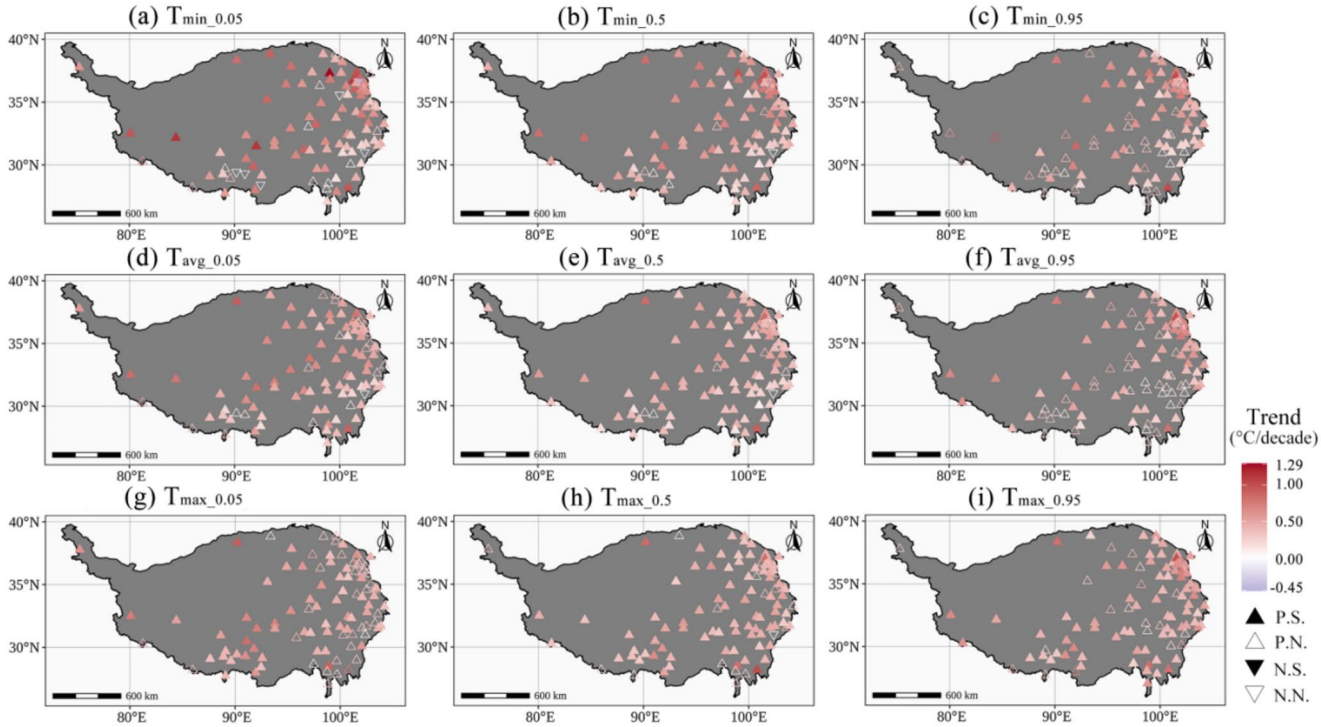

Figure 4. Spatial distribution of quantile regression at meteorological stations over Tibetan Plateau (TP) from 1979 to 2019, (a–c) for $T_{min\_0.05}$, $T_{avg\_0.05}$, and $T_{max\_0.05}$ (d–f) for $T_{min\_0.5}$, $T_{avg\_0.5}$, and $T_{max\_0.5}$, (g–i) for $T_{min\_0.95}$, $T_{avg\_0.95}$, and $T_{max\_0.95}$, respectively. In legend, P.S. and N.S. respectively represent significantly positive and negative trend at 0.05 significant level, whereas P.N. and N.N. correspond to P.S. and N.S. but for insignificant trend.

4.2. Warming Trend Comparison

Many studies have demonstrated that the TP is warming significantly and one of the general conclusions is that the warming rate of T_{min} is higher than that of T_{max} (Liu et al., 2006; Li et al., 2010; Xie et al., 2010; Hu et al., 2011; Liu et al., 2011; You, Min, Jiao, et al., 2016, You, Min, Kang, et al., 2016). Similar results are revealed in this study, for example, the trend of T_{min}, T_{avg}, and T_{max} from 1979 to 2019 are respectively 0.47, 0.38, and 0.41°C/decade at 0.5 quantile (Table 2), however, differences in the change rate can be expected due to different time periods and methods involved in the analysis. For example, the warming trend of T_{min} is even greater than T_{max} during 1961–2003 with the corresponding trend of 0.41°C/decade and 0.18°C/decade (Liu et al., 2006). It is likely because the time period used in this study is 1979–2019 and all daily data are involved in the analysis rather than synthesizing daily data into annual. A recent study showed that the average trends in annual maximum daily maximum temperature and in annual minimum daily minimum temperature on the TP are 0.59 and 0.37°C/decade during 1973–2018 (Yang et al., 2022), which is close to our results of 0.51°C/decade in extremely cold days of T_{min} and 0.46°C/decade in extremely hot days of T_{max} (Table 2). Our findings that extremely cold days change faster than extremely hot day are similar to the study conducted in the daily mean temperature time series in China (Gao & Franzke, 2017), which is also practicable for T_{min} but opposite for T_{max}. However, the rate difference between extremely cold days and extremely hot days is relatively smaller than the result for China (Gao & Franzke, 2017), which is probably because that climate warming on the TP is much higher and is reaching a regionally critical value. In spatial terms, our results also indicate the magnitude of temperature warming increases from south to north spatially, which is consistent with the previous studies (Guo & Wang, 2012; Li et al., 2010; Xie et al., 2010; You, Min, Jiao, et al., 2016). Nevertheless, more meteorological sites appear to show insignificant change in extremely hot days than in extremely cold days for all the temperature variables (Figure 4). This spatially site-scale variability prompts us to analyze the elevation dependence of extreme temperature change at different quantile levels.

10.1029/2022EA002571

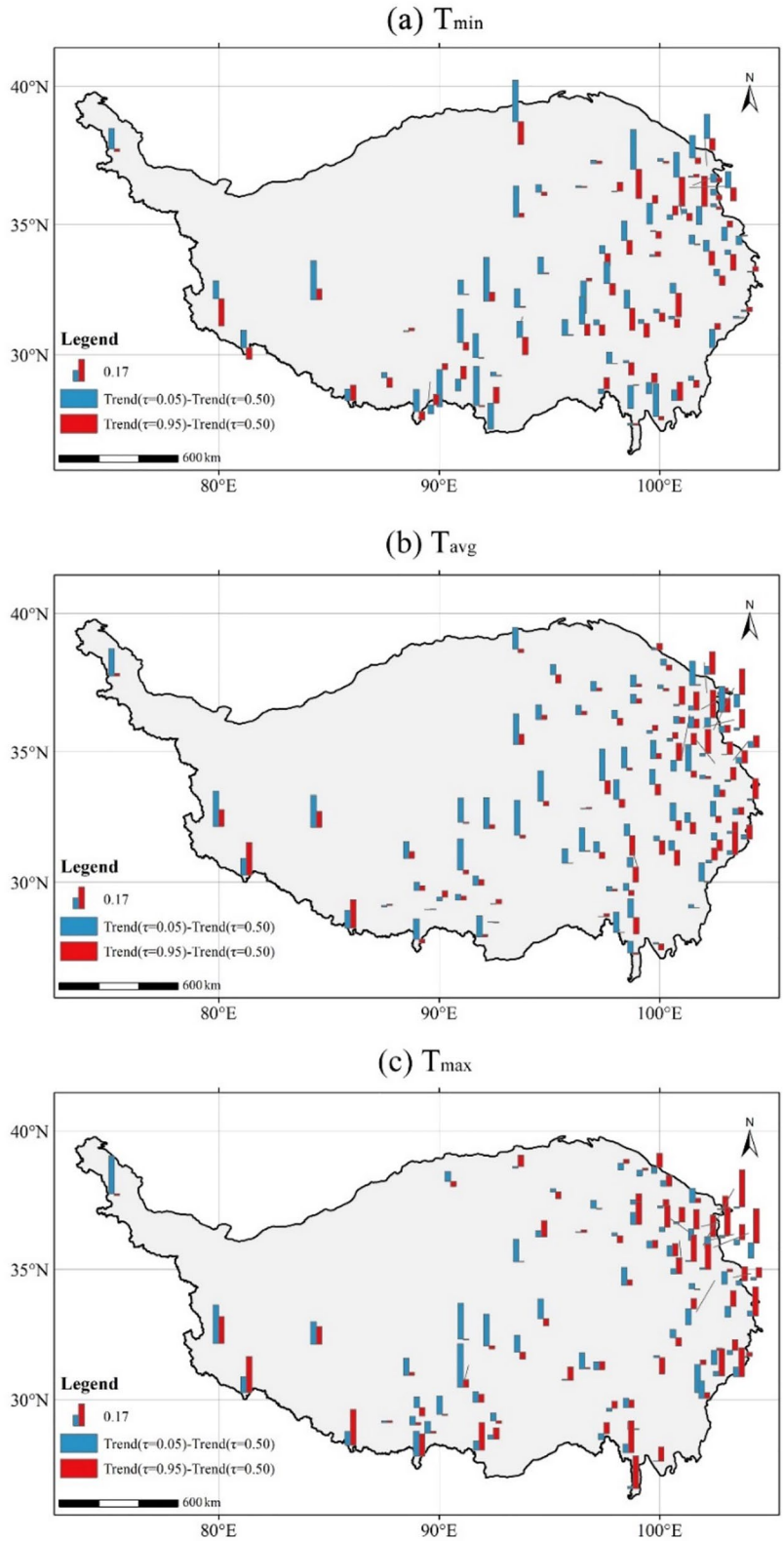

Figure 5. The trend symmetry of extremely cold ($\tau = 0.05$) and hot days ($\tau = 0.95$) using mean condition ($\tau = 0.5$) as a reference for (a) T_{min}, (b) T_{avg}, (c) T_{max}.

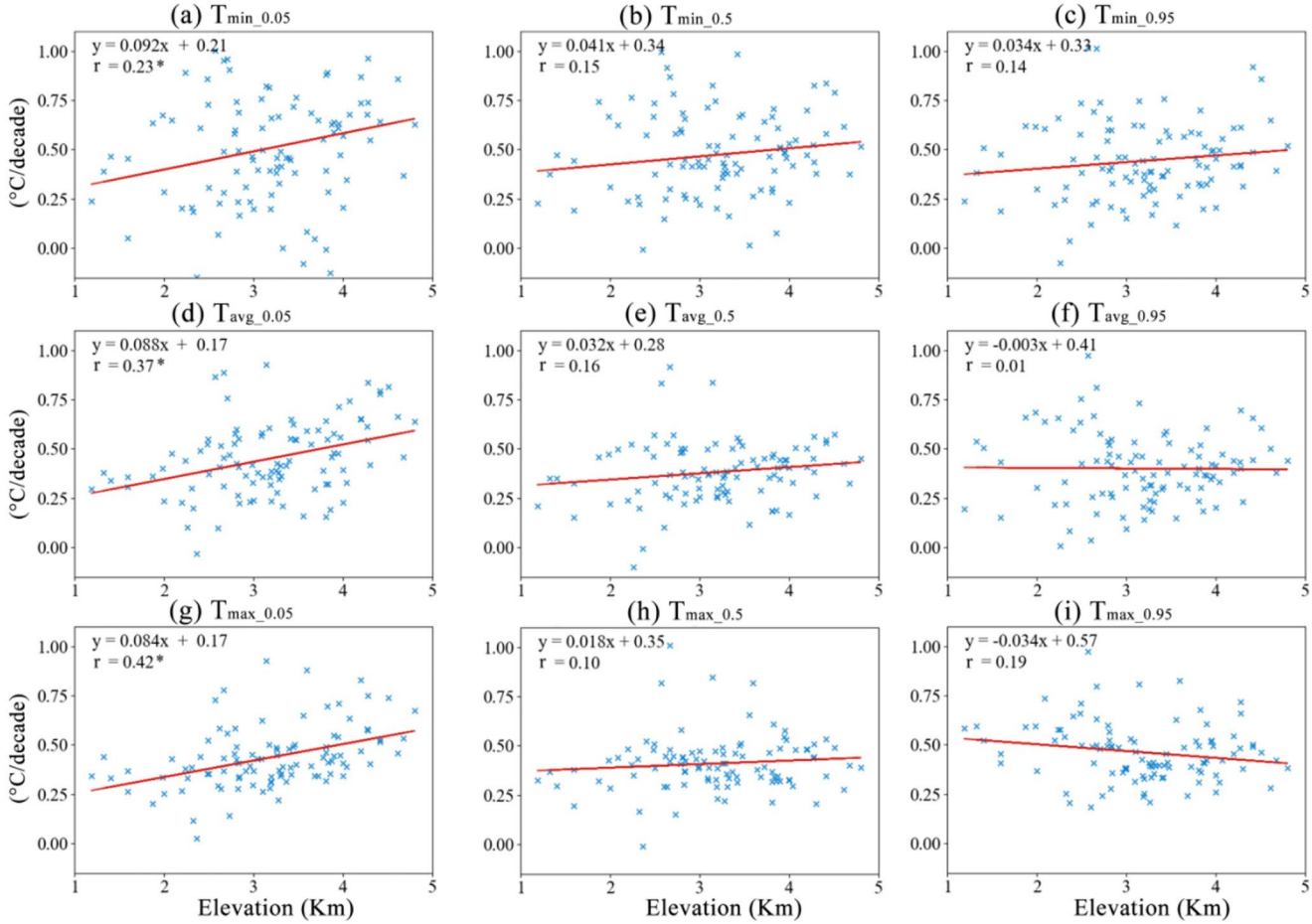

Figure 6. Relationship between elevation and quantile regression trends from 1979 to 2019 of (a–c) $T_{min\_0.05}$, $T_{avg\_0.05}$, and $T_{max\_0.05}$ (d–f) $T_{min\_0.5}$, $T_{avg\_0.5}$, and $T_{max\_0.5}$ and (g–i) $T_{min\_0.95}$, $T_{avg\_0.95}$, and $T_{max\_0.95}$. An asterisk means significant trend at 0.05 significant level and r represents correlation coefficient.

4.3. The Mechanisms and Altitude Dependence Exploration

Previous work showed that the warming rate of annual-composited minimum temperature increased with elevation on the TP during the period of both 1961–2005 (You, Kang, Pepin, et al., 2008) and 1973–2018 (Yang et al., 2022). This study witnesses a similar result for the warming trend of extremely cold days in the three temperature time series from 1979 to 2019 (Figure 4). On the contrary, our work shows that insignificant elevation-dependency of the warming trend in both mean condition and extremely hot days from 1979 to 2019 (Figure 5) is similar to the result of annual-composited maximum temperature during 1973–2018 (Yang et al., 2022). This may partly be related to the fact that the warming trend of the extremely cold days is stronger than that of the mean condition and extremely hot days (Qin et al., 2009), however, in the case of T_{max}, it is possibly due to more sites with insignificant warming (Table 2). In addition, the significance of elevation dependency greatly relies on the temporal evolution. For instance, elevation dependency of annual-composited minimum temperature is insignificant in earlier years but has become significant more recently (Yang et al., 2022). It is also important to note that most of the available stations in this study are mainly located in eastern valleys, while the western part is poorly represented and this could affect results when using data only gathered by meteorological stations. Fortunately, satellite observations with wall-to-wall coverage show great potential for detecting the temperature extremes warming in the TP region, however, the sporadic cloud contamination to optical remote sensing probably restricts to capture the extreme observation, hence more work is required to evaluate, calibrate and integrate satellite data (Zhang et al., 2021). Finally, the overall regional-effects of two large-scale climate patterns (ENSO and AO) on temperature extremes are investigated at the three clusters over the TP based on quantile regression. Past studies have demonstrated that the influence of ENSO and AO on mainland China exhibited distinctly regional and seasonal characteristics, which respectively is closely linked with the summer and winter temperature extreme at

10.1029/2022EA002571

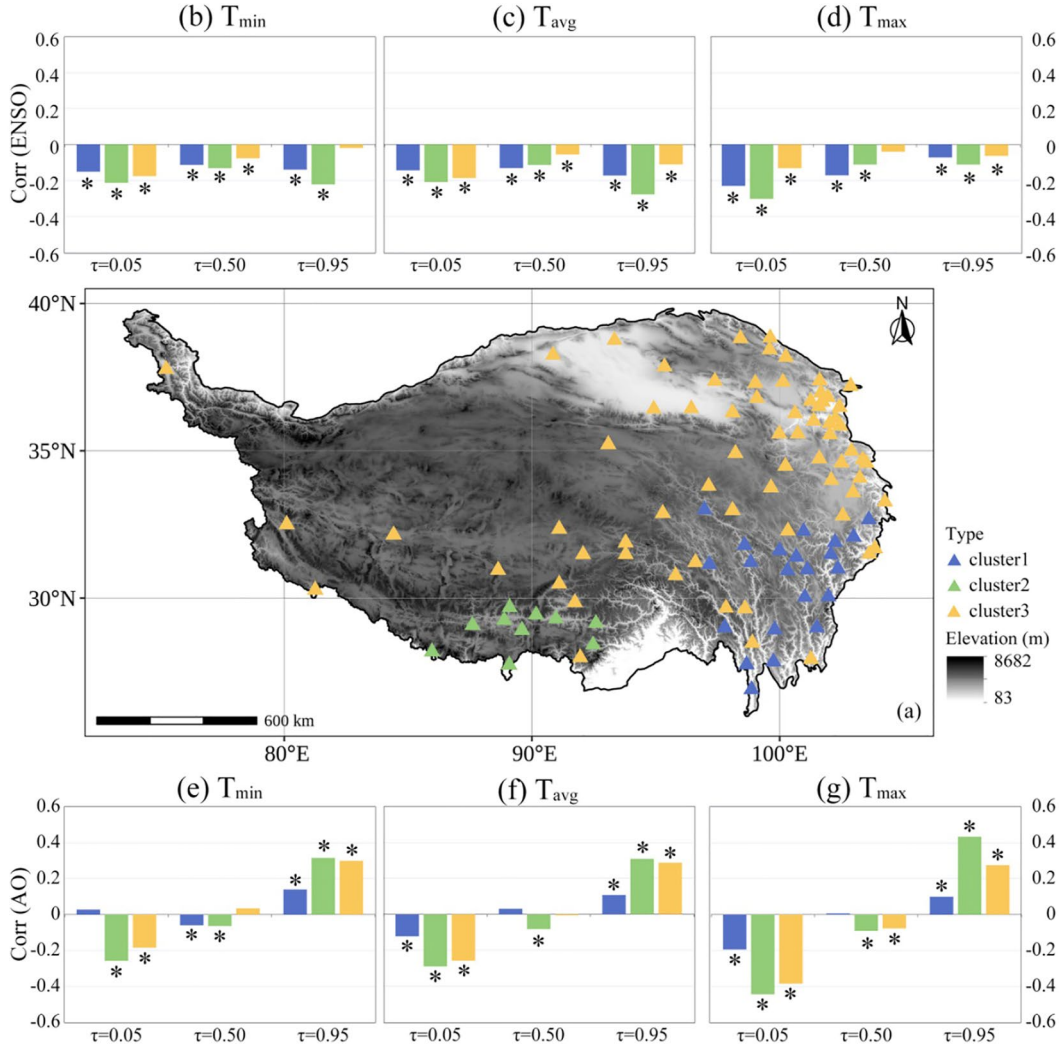

Figure 7. K-Nearest Neighbor (KNN)-derived (a) spatial clustering result by simultaneously inputting quantile trends of the daily minimum, mean and maximum temperature from 1979 to 2019 at quantile levels of 0.05, 0.5, 0.95 and the potential teleconnection analysis between climate index and the corresponding temperature serial, including (b–d) the El Niño–Southern Oscillation (ENSO) and (e–g) the Arctic Oscillation (AO). An asterisk means significant trend at 0.05 significant level.

interannual scale (Chen et al., 2013; Gong & Wang, 2003; Lin & Lu, 2009). In this study, the north-south heterogeneity of the teleconnection is also found on the TP. Specifically, the AO has a more significant influence on the warming of extremely cold days (negative influence) and hot days (positive influence) occurring on the northern and southwestern regions (C2 and C3). This finding coincides with Meng's study (Gao & Franzke, 2017) which shows that cold extremes is strongly associated with the AO in northern China. In particular, the negative and positive impact is also consistent when we take into account the teleconnection analysis on meteorological stations on the TP in Gao's study (Gao & Franzke, 2017). With respect to ENSO, its overall impact on the change in extreme temperature is comparable smaller than AO, however, the mechanisms of climate warming on the TP are so complex that it is still not fully understood. Snow/ice-albedo feedback (Liu & Chen, 2000), cloud change (Duan & Wu, 2006) and surface water vapor (Rangwala et al., 2009) are all likely to influence climate warming on the TP, therefore, a comprehensive investigation of the mechanical linkage combining the atmospheric circulation and local environment and their joint influences on climate extremes on the TP is worthwhile.

5. Conclusion

This study provided a comprehensive investigation of changes in temperature extremes from 1979 to 2019 (T_{min}, T_{avg}, and T_{max}) based on the quantile regression method at 100 meteorological stations over the TP. The widespread existence of long-range dependence at most of meteorological stations enabled us to apply 1000 surrogate time series for detecting the statistical significance of the quantile trends. The trends of T_{min}, T_{mean}, and T_{max} were with intervals of [−0.45, 1.29], [−0.1, 0.98], [−0.01, 1.01]°C/decade respectively among conditional quantile levels. Overall, T_{min} was warming faster than T_{max} and T_{mean} at 0.05 and 0.5 quantile level, but the trend of T_{max} reached maximum at 0.95 quantile level. Meanwhile, the warming rate of extremely cold days ($\tau = 0.05$) and hot days ($\tau = 0.95$) was higher than that of mean condition ($\tau = 0.5$). Altitude dependence of climate warming was explored and found that it is significant in extremely cold days but insignificant in extremely hot days and mean weather conditions. In addition, we also found that the AO strongly correlated with extreme cold and hot days over the northern and southwestern TP region, while the ENSO mainly modulated temperatures over the southeastern TP area. This study may improve our understanding of temperature extremes across the TP and is critical for assessing the ecohydrological process and associated hazards.

Data Availability Statement

The daily temperature data are provided by from National Meteorological Information Center (National Meteorological Information Center, 2019): https://agupubs.onlinelibrary.wiley.com/doi/full/10.1029/2022EA002232. The topography data [Global 30 Arc-Second Elevation (GTOPO30)] can be obtained from the U.S. Geological Survey: https://doi.org/10.5066/F7DF6PQS. The daily El Niño–Southern Oscillation and Arctic Oscillation data are respectively provided by NOAA Physical Sciences Laboratory and NOAA National Weather Service Climate Prediction Center: https://www.psl.noaa.gov/data/gridded/data.noaa.oisst.v2.highres.html and https://www.cpc.ncep.noaa.gov/products/precip/CWlink/daily_ao_index/ao.shtml.

Acknowledgments
The authors declare no conflicts of interest. This work was supported by the Third Xinjiang Scientific Expedition Program (2021xjkk130301), and the Key Special Project for Introduced Talents Team of Southern Marine Science and Engineering Guangdong Laboratory (Grand GML2019ZD0301), supported by the National Natural Science Foundation of China Grand 42201053 and a grant from State Key Laboratory of Resources and Environmental Information System. The authors would like to thank "National Earth System Science Data Center, National Science & Technology Infrastructure of China" for the data support (http://www.geodata.cn).

References

Alexander, L. V., Zhang, X., Peterson, T. C., Caesar, J., Gleason, B., Klein, T., et al. (2006). Global observed changes in daily climate extremes of temperature and precipitation. *Journal of Geophysical Research*, *111*(5), 1–22. https://doi.org/10.1029/2005JD006290

Barbosa, S. M., Scotto, M. G., & Alonso, A. M. (2011). Summarising changes in air temperature over Central Europe by quantile regression and clustering. *Natural Hazards and Earth System Sciences*, *11*(12), 3227–3233. https://doi.org/10.5194/nhess-11-3227-2011

Brown, S. J., Caesar, J., & Ferro, C. A. T. (2008). Global changes in extreme daily temperature since 1950. *Journal of Geophysical Research*, *113*(5), 1–11. https://doi.org/10.1029/2006JD008091

Chen, S., Chen, W., & Wei, K. (2013). Recent trends in winter temperature extremes in eastern China and their relationship with the Arctic oscillation and ENSO. *Advances in Atmospheric Sciences*, *30*(6), 1712–1724. https://doi.org/10.1007/s00376-013-2296-8

Cui, P., Chen, R., Xiang, L., & Su, F. (2014). Risk analysis of mountain hazards in Tibetan Plateau under global warming. *Advances in Climate Change Research*, *10*(2), 103–109. https://doi.org/10.3969/j.issn.1673-1719.2014.02.004

Ding, J., Cuo, L., Zhang, Y., & Zhu, F. (2018). Monthly and annual temperature extremes and their changes on the Tibetan Plateau and its surroundings during 1963–2015. *Scientific Reports*, *8*(1), 1–23. https://doi.org/10.1038/s41598-018-30320-0

Duan, A., & Wu, G. (2006). Change of cloud amount and the climate warming on the Tibetan Plateau. *Geophysical Research Letters*, *33*(22), 1–5. https://doi.org/10.1029/2006GL027946

Duan, A., & Xiao, Z. (2015). Does the climate warming hiatus exist over the Tibetan Plateau? *Scientific Reports*, *5*, 1–9. https://doi.org/10.1038/srep13711

Duan, Q., McGrory, C. A., Brown, G., Mengersen, K., & Wang, Y.-G. (2021). Spatio-temporal quantile regression analysis revealing more nuanced patterns of climate change: A study of long-term daily temperature in Australia. ArXiv Preprint ArXiv, 2103.05791 Retrieved from http://arxiv.org/abs/2103.05791

Fan, F., Liu, Y., Chen, J., & Dong, J. (2021). Scenario-based ecological security patterns to indicate landscape sustainability: A case study on the qinghai-Tibet plateau. *Landscape Ecology*, *36*(7), 2175–2188. https://doi.org/10.1007/s10980-020-01044-2

Fatichi, S., Barbosa, S. M., Caporali, E., & Silva, M. E. (2009). Deterministic versus stochastic trends: Detection and challenges. *Journal of Geophysical Research*, *114*(18), 1–11. https://doi.org/10.1029/2009JD011960

Feldstein, S. B., & Franzke, C. L. E. (2017). Atmospheric teleconnection patterns. In *Nonlinear and stochastic climate dynamics* (pp. 54–104). Cambridge University Press. https://doi.org/10.1017/9781316339251.004

Franzke, C. (2010). Long-range dependence and climate noise characteristics of Antarctic temperature data. *Journal of Climate*, *23*(22), 6074–6081. https://doi.org/10.1175/2010JCLI3654.1

Franzke, C. (2012). Nonlinear trends, long-range dependence, and climate noise properties of surface temperature. *Journal of Climate*, *25*(12), 4172–4183. https://doi.org/10.1175/JCLI-D-11-00293.1

Franzke, C. (2013). A novel method to test for significant trends in extreme values in serially dependent time series. *Geophysical Research Letters*, *40*(7), 1391–1395. https://doi.org/10.1002/grl.50301

Gao, M., & Franzke, C. L. E. (2017). Quantile regression-based spatiotemporal analysis of extreme temperature change in China. *Journal of Climate*, *30*(24), 9897–9914. https://doi.org/10.1175/JCLI-D-17-0356.1

Geweke, J., & Porter-Hudak, S. (1983). The estimation and application of long memory time series models. *Journal of Time Series Analysis*, *4*(4), 221–238. https://doi.org/10.1111/j.1467-9892.1983.tb00371.x

Gong, D., & Wang, S. (2003). Influence of Arctic oscillation on winter climate over China. *Dili Xuebao/Acta Geographica Sinica*, *58*(4), 568–575. https://doi.org/10.1007/bf02837460

Granger, C. W. J., & Joyeux, R. (1980). An introduction to longmemory time series models and fractional differencing. *Journal of Time Series Analysis*, *1*, 15–29. https://doi.org/10.1111/j.1467-9892.1980.tb00297.x

Grimaldi, S. (2004). Linear parametric models applied to daily hydrological series. *Journal of Hydrologic Engineering*, *9*(5), 383–391. https://doi.org/10.1029/2009JD011960

Guo, D., & Wang, H. (2012). The significant climate warming in the northern Tibetan Plateau and its possible causes. *International Journal of Climatology*, *32*(12), 1775–1781. https://doi.org/10.1002/joc.2388

Hosking, J. R. M. (1981). Fractional differencing. *Biometrika*, *68*(1), 165–176. https://doi.org/10.1093/biomet/68.1.165

Hu, Y., Maskey, S., Uhlenbrook, S., & Zhao, H. (2011). Streamflow trends and climate linkages in the source region of the Yellow River, China. *Hydrological Processes*, *25*(22), 3399–3411. https://doi.org/10.1002/hyp.8069

Kenyon, J., & Hegerl, G. C. (2008). Influence of modes of climate variability on global temperature extremes. *Journal of Climate*, *21*(15), 3872–3889. https://doi.org/10.1175/2008JCLI2125.1

Kharin, V. V., Zwiers, F. W., Zhang, X., & Hegerl, G. C. (2007). Changes in temperature and precipitation extremes in the IPCC ensemble of global coupled model simulations. *Journal of Climate*, *20*(8), 1419–1444. https://doi.org/10.1175/JCLI4066.1

Kharin, V. V., Zwiers, F. W., Zhang, X., & Wehner, M. (2013). Changes in temperature and precipitation extremes in the CMIP5 ensemble. *Climatic Change*, *119*(2), 345–357. https://doi.org/10.1007/s10584-013-0705-8

Koenker, R., & Bassett, G. (1978). Regression quantiles. *Econometrica*, *46*(1), 33–50. https://doi.org/10.2307/1913643

Koenker, R., & Schorfheide, F. (1994). Quantile spline models for global temperature change. *Climatic Change*, *28*(4), 395–404. https://doi.org/10.1007/BF01104081

Lan, X., Li, W., Tang, J., Zhao, F., & Fan, J. (2022). Spatiotemporal variation of climate of different flanks and elevations of the Qinling–Daba Mountains in China during 1969–2018. *Scientific Reports*, *12*(1), 6952. https://doi.org/10.1038/s41598-022-10819-3

Li, L., Yang, S., Wang, Z., Zhu, X., & Tang, H. (2010). Evidence of warming and wetting climate over the Qinghai-Tibet plateau. *Arctic Antarctic and Alpine Research*, *42*(4), 449–457. https://doi.org/10.1657/1938-4246-42.4.449

Lin, Z., & Lu, R. (2009). The ENSO's effect on eastern China rainfall in the following early summer. *Advances in Atmospheric Sciences*, *26*(2), 333–342. https://doi.org/10.1007/s00376-009-0333-4

Liu, X., & Chen, B. (2000). Climatic warming in the Tibetan Plateau during recent decades. *International Journal of Climatology*, *20*(14), 1729–1742. https://doi.org/10.1002/1097-0088(20001130)20:14<1729:AID-JOC556>3.0.CO;2-Y

Liu, X., Cheng, Z., Yan, L., & Yin, Z. Y. (2009). Elevation dependency of recent and future minimum surface air temperature trends in the Tibetan Plateau and its surroundings. *Global and Planetary Change*, *68*(3), 164–174. https://doi.org/10.1016/j.gloplacha.2009.03.017

Liu, X., Yin, Z. Y., Shao, X., & Qin, N. (2006). Temporal trends and variability of daily maximum and minimum, extreme temperature events, and growing season length over the eastern and central Tibetan Plateau during 1961-2003. *Journal of Geophysical Research*, *111*(19), 1–19. https://doi.org/10.1029/2005JD006915

Liu, X., Zheng, H., Zhang, M., & Liu, C. (2011). Identification of dominant climate factor for pan evaporation trend in the Tibetan Plateau. *Journal of Geographical Sciences*, *21*(4), 594–608. https://doi.org/10.1007/s11442-011-0866-1

National Meteorological Information Center. (2019). Daily meteorological dataset of basic meteorological elements of China National Surface Weather Station (V3.0) (1951–2010) [Dataset]. National Tibetan Plateau Data Center. Retrieved from https://data.tpdc.ac.cn/en/data/52c77e9c-df4a-4e27-8e97-d363fdfce10a/

Pepin, N., Bradley, R. S., Diaz, H. F., Baraer, M., Caceres, E. B., Forsythe, N., et al. (2015). Elevation-dependent warming in mountain regions of the world. *Nature Climate Change*, *5*(5), 424–430. https://doi.org/10.1038/nclimate2563

Qin, J., Yang, K., Liang, S., & Guo, X. (2009). The altitudinal dependence of recent rapid warming over the Tibetan Plateau. *Climatic Change*, *97*(1), 321–327. https://doi.org/10.1007/s10584-009-9733-9

Ramos, A. M., Lorenzo, M. N., & Gimeno, L. (2010). Compatibility between modes of low-frequency variability and circulation types: A case study of the northwest Iberian Peninsula. *Journal of Geophysical Research*, *115*(D2), D02113. https://doi.org/10.1029/2009JD012194

Rangwala, I., Miller, J. R., & Xu, M. (2009). Warming in the Tibetan Plateau: Possible influences of the changes in surface water vapor. *Geophysical Research Letters*, *36*(6), 1–6. https://doi.org/10.1029/2009GL037245

Schreiber, T., & Schmitz, A. (1996). Improved surrogate data for nonlinearity tests. *Physical Review Letters*, *77*(4), 635–638. https://doi.org/10.1103/PhysRevLett.77.635

Screen, J. A. (2014). Arctic amplification decreases temperature variance in northern mid-to high-latitudes. *Nature Climate Change*, *4*(7), 577–582. https://doi.org/10.1038/nclimate2268

Wang, S., Zhang, M., Wang, B., Sun, M., & Li, X. (2013). Recent changes in daily extremes of temperature and precipitation over the Western Tibetan Plateau, 1973-2011. *Quaternary International*, *313*, 110–117. https://doi.org/10.1016/j.quaint.2013.03.037

Xie, H., Ye, J., Liu, X., & Chongyi, E. (2010). Warming and drying trends on the Tibetan Plateau (1971-2005). *Theoretical and Applied Climatology*, *101*(3), 241–253. https://doi.org/10.1007/s00704-009-0215-9

Xue, Y., Chen, Q., Zhang, J., & Huang, P. (2020). Trends in extreme high temperature at different altitudes of Southwest China during 1961–2014. *Atmospheric and Oceanic Science Letters*, *13*(5), 417–425. https://doi.org/10.1080/16742834.2020.1799689

Yan, Y., & Tang, Z. (2019). Protecting endemic seed plants on the Tibetan Plateau under future climate change: Migration matters. *Journal of Plant Ecology*, *12*(6), 962–971. https://doi.org/10.1093/jpe/rtz032

Yang, K., Guo, D., Hua, W., Pepin, N., Yang, K., & Li, D. (2022). Tibetan plateau temperature extreme changes and their elevation dependency from ground-based observations. *Journal of Geophysical Research: Atmospheres*, *127*(3), e2021JD035734. https://doi.org/10.1029/2021JD035734

Yao, T., Thompson, L., Yang, W., Yu, W., Gao, Y., Guo, X., et al. (2012). Different glacier status with atmospheric circulations in Tibetan Plateau and surroundings. *Nature Climate Change*, *2*(9), 663–667. https://doi.org/10.1038/nclimate1580

Yin, H., Sun, Y., & Donat, M. G. (2019). Changes in temperature extremes on the Tibetan Plateau and their attribution. *Environmental Research Letters*, *14*(12), 124015. https://doi.org/10.1088/1748-9326/ab503c

You, Q., Kang, S., Aguilar, E., Pepin, N., Flugel, W. A., Yan, Y., et al. (2011). Changes in daily climate extremes in China and their connection to the large scale atmospheric circulation during 1961-2003. *Climate Dynamics*, *36*(11), 2399–2417. https://doi.org/10.1007/s00382-009-0735-0

You, Q., Kang, S., Aguilar, E., & Yan, Y. (2008). Changes in daily climate extremes in the eastern and central Tibetan Plateau during 1961-2005. *Journal of Geophysical Research*, *113*(7), 1–17. https://doi.org/10.1029/2007JD009389

You, Q., Kang, S., Pepin, N., & Yan, Y. (2008). Relationship between trends in temperature extremes and elevation in the eastern and central Tibetan Plateau, 1961-2005. *Geophysical Research Letters*, *35*(4), 1–7. https://doi.org/10.1029/2007GL032669

You, Q., Min, J., Jiao, Y., Sillanpää, M., & Kang, S. (2016). Observed trend of diurnal temperature range in the Tibetan plateau in recent decades. *International Journal of Climatology*, *36*(6), 2633–2643. https://doi.org/10.1002/joc.4517

You, Q., Min, J., & Kang, S. (2016). Rapid warming in the Tibetan plateau from observations and CMIP5 models in recent decades. *International Journal of Climatology*, *36*(6), 2660–2670. https://doi.org/10.1002/joc.4520

Zhang, L., Guo, H. D., Wang, C. Z., Ji, L., Li, J., Wang, K., & Dai, L. (2014). The long-term trends (1982-2006) in vegetation greenness of the alpine ecosystem in the Qinghai-Tibetan Plateau. *Environmental Earth Sciences*, *72*(6), 1827–1841. https://doi.org/10.1007/s12665-014-3092-1

Zhang, W., Ren, Z., Yao, L., Zhou, C., & Zhu, Y. (2016). Numerical modeling and prediction of future response of permafrost to different climate change scenarios on the Qinghai–Tibet Plateau. *International Journal of Digital Earth*, *9*(5), 442–456. https://doi.org/10.1080/17538947.2015.1041431

Zhang, W., Zhang, B., Zhu, W., Tang, X., Li, F., Liu, X., & Yu, Q. (2021). Comprehensive assessment of MODIS-derived near-surface air temperature using wide elevation-spanned measurements in China. *Science of the Total Environment*, *800*, 149535. https://doi.org/10.1016/j.scitotenv.2021.149535

Zhu, F., Gao, J., Yang, J., & Ye, N. (2022). Neighborhood linear discriminant analysis. *Pattern Recognition*, *123*, 108422. https://doi.org/10.1016/j.patcog.2021.108422